

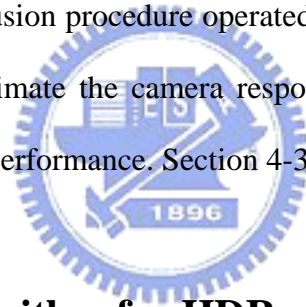
# Chapter 4

## Proposed Image Fusion Algorithm for HDR

---

### 4.1 Introduction

Scenes from the real world exhibit a wide dynamic range especially outdoors with shadow or indoors with a sunlit window. However, it is impossible for digital still camera (DSC) to prevent information loss under bright and dim ambient. The reliable method is to combine multiple images of the same scene with different exposures introduced in section 2.3 [8-9], [15]. Section 4-2 will be our fusion procedure operated in raw data image. Moreover, we will simplify the processing to estimate the camera response curve and modify the appropriate weighting curve for preferred performance. Section 4-3 will be the summary.



### 4.2 Our Fusion Algorithm for HDR

Our Fusion Algorithm for high dynamic range was operated by 12-bit raw image and the camera response curve, and the weighting functions were estimated as well. In the following sections, the main techniques including response curve, weighting function, and combination will be introduced. In addition, some issues among above techniques will be discussed and improved by our proposed model. Each section will be divided into three parts: previous method, discussions, and improved method.

#### 4.2.1 Camera Response Curve

##### (a) Previous method:

The camera response curve is a transformation between the pixel values  $f(q)$  and the photo

quantity ( $q$ ). Among all proposed approximate camera response curves [15], the most flexible model is expressed as equation 4-1.

$$f(q) = \frac{1}{(1 + \exp\{-[A \log(q)]\})^c} \quad (4-1)$$

where the unknowns are the parameters  $A$  and  $C$ . The pixel values  $f(q)$  were normalized to the range  $[0:1]$ . Parametric estimation can be performed by using the following observation: two different images of the same scene with different exposed times and the exposure ratio ( $k$ ) between them. It is possible to derive the following equation 4-2:

$$g[f(q)] = f(kq) \quad (4-2)$$

where  $g$  was a new unknown function expressing how a pixel value of the first image becomes a new pixel value in the second one. This relationship could be easily observed by building up a *cross-histogram* of the two images: a  $4096 \times 4096$  plot where an entry at position  $(x,y)$  means that the gray level  $x$  of the low exposed image becomes the gray level  $y$  of high exposed image. The equation 4-3 was induced by combining equations 4-1 and 4-2. The equation was called the *comparametric equation* [15].

$$g(f) = \frac{fk^{ac}}{(\sqrt[c]{f}(k^a - 1) + 1)^c} \quad (4-3)$$

By the cross-histogram, the pair values  $(f(q), g[f(q)])$  were known, parameters  $A$  and  $C$  could be retrieved by means of nonlinear regression across well populated pairs. Once  $A$  and

C were estimated, the camera response curve was achieved. There are many camparametric equations and response curves are listed in **Table 4-1**. Different equations will result in different effects.

**Table 4-1 List the useful examples of camparametric equations and their solutions which are also the camera response curves [15].**

Comparametric equation	Solution (camera response curve)
$g[f(q)] = f(kq)$	<b>f(q)</b>
$g = f^\gamma$	$f = \exp(q^\Gamma), \quad \gamma = k^\Gamma$
$g = k^\gamma f$	$f = q^\gamma$
$g = af + b, \quad \forall a \neq 1, \text{ or } b=0$	$f = \alpha + \beta q^\gamma, a = k^\gamma, \quad b = \alpha(1 - k^\gamma)$
$g = f + b,$	$f = B \log(\beta q), b = B \log k$
$g = (\sqrt[\zeta]{f} + \log k)^\gamma$	$f = \log^\gamma q$
$g = \begin{cases} ((2^\zeta - 1)f + 1)^{\frac{1}{\zeta}} - 1, & \forall \zeta \neq 1 \\ 2^f - 1, & \text{for } \zeta = 0 \end{cases}$	$\frac{e^q - 1}{2^\zeta - 1}$
$g = e^b f^a = e^{\alpha(1-k^\gamma)} f^{(k^\gamma)}$	$f = \alpha + \beta q^\gamma$
$g = \exp((\log f)^{(k^b)})$	$f = \exp(a^{(q^b)})$
$g = \exp(\log^k f)$	$f = \exp(a^{bq})$
$g = \frac{2}{\pi} \arctan(k \tan(\frac{2}{\pi} f))$	$f = \frac{2}{\pi} \arctan(q)$
$g = \frac{1}{\pi} \arctan(b\pi \log k + \tan((f - \frac{1}{2})\pi) + \frac{1}{2})$	$f = \begin{cases} \frac{1}{\pi} \arctan(b\pi \log q) + \frac{1}{2}, & \forall q \neq 0 \\ 0, & \text{for } q = 0 \end{cases}$
$g = \frac{fk^{ac}}{(\sqrt[\zeta]{f(k^a - 1) + 1})^c}$	$f = \left( \frac{e^b q^a}{e^b q^a} \right)^c = \begin{cases} \left( \frac{1}{1 + e^{-(a \log q + b)}} \right)^c, & \forall q \neq 0 \\ 0, & \text{for } q = 0 \end{cases}$
$g = \exp\left( \frac{\sqrt[\zeta]{\log f k^{ac}}}{(\sqrt[\zeta]{\log f (k^a - 1) + 1})^c} \right)$	$f = \exp\left( \left( \frac{e^b q^a}{e^b q^a} \right)^c \right) = \begin{cases} \exp\left( \left( \frac{1}{1 + e^{-(a \log q + b)}} \right)^c \right), & \forall q \neq 0 \\ 0, & \text{for } q = 0 \end{cases}$

**(b)Discussions:**

It is necessary to compute the relative position in cross-histogram to obtain the comparametric equation. However, too huge (896×1408 pixels) image size causes the great complexity because of a large number of samples. Moreover, the random noise of both two images causes unreliable relative position.

**(c)The improved method:**

Using mean value of block contained 5x5 pixels can simplify the computation. The uniform block is defined by its standard deviation expressed as equation 4-4 within 0.01.

$$\sigma = \sqrt{\frac{\sum_{i=1}^n (x_i - \bar{x})^2}{n}} \quad (4-4)$$

$\bar{x}$  and n are the mean value and the samples of this block respectively. Our improved method not only speed the algorithm but also reduce the effect of noise which can be suppressed by averaging. Two images were taken by the camera Nikon D70 with different exposures and the exposure ration (k) is 4. High and low exposed images are shown in **Figs. 4-1 (a)** and **(b)** respectively. The cross-histogram of comparametric equation is shown in **Fig. 4-2**.

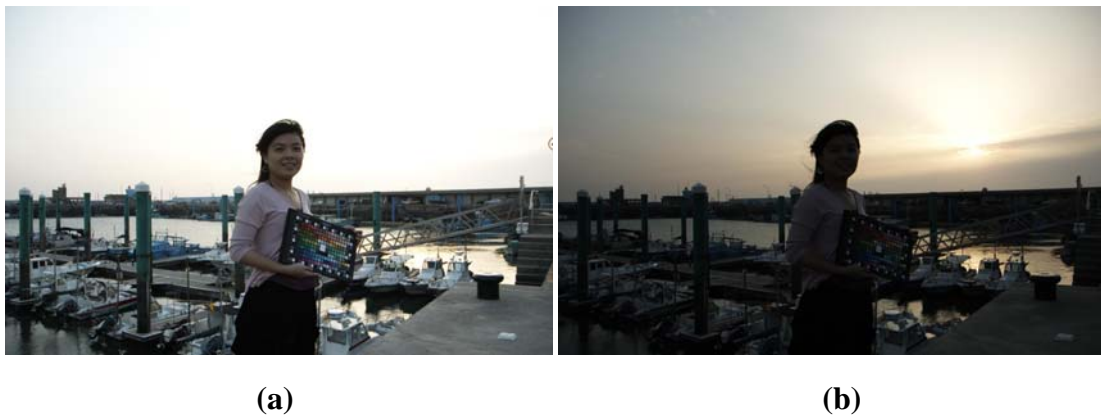


**Fig. 4-1 Two images with different exposures. (a) High exposure and (b) low exposure.**

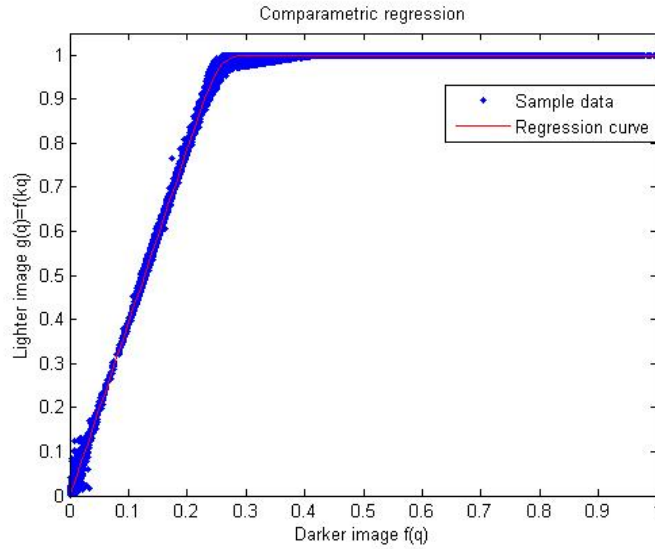


**Fig. 4-2 The cross-histogram of comparametric equation.**

The dots are the samples of two images and the line is the nonlinear regression. From the result of comparametric equation, it is found that  $A=23.05$  and  $C=0.042$ . Therefore, the camera response curve illustrated in Fig. 4-3 is derived by equation 4-1. The curve of high exposure is shifted the value,  $\log(k)$ , along the - vertical axis because the high exposed image are of a factor of  $k$  larger than the low exposed image in  $q$  domain. In  $\log(q)$  domain, it is equal to subtract  $\log(k)$ .

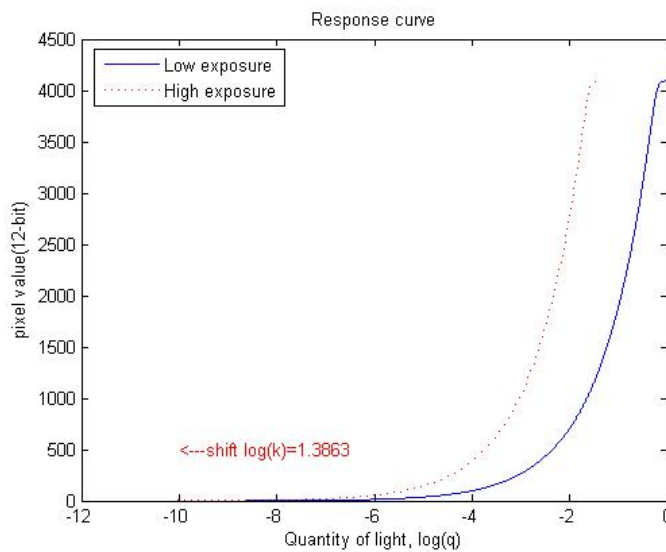


**Fig. 4-3 The camera response curve. Vertical axis is the pixel values with 12-bits and parallel axis is  $\log(q)$ .**

## 4.2.2 Weighting Function

### (a) Previous method:

The weighting function is the slope of the camera response curve which indicates how quickly the output (pixel value) of the camera varies for given input. Therefore, the differential of response curve is taken as previous weighting function. The weighting function of low exposed image which varies from  $q$  and  $\log q$  is shown in **Fig. 4-4** and **Fig. 4-5**. The weighting function of high one in **Fig. 4-4** is to be shifted  $\log(k)$  along left direction and in **Fig. 4-5** is to be divided by 4 times.

### (b) Discussions:

For the weighting function with high exposure in **Fig. 4-5**, the slope of high  $q$  (right side) is sharp which leads to discontinuous surface of the weighting image. The weighting image normalized to 8-bits of **Fig. 4-1 (a)** is shown in **Fig. 4-6** which illustrates a discontinuous region in high pixel values (sky).

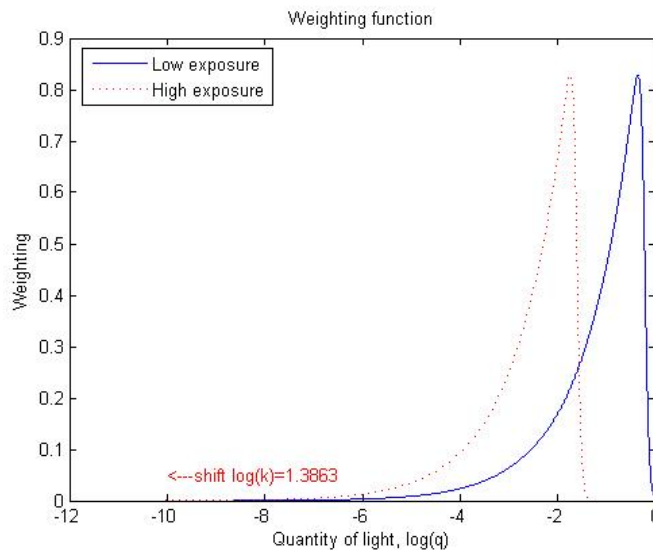


**Fig. 4-4** The weighting functions of low and high exposures respectively.

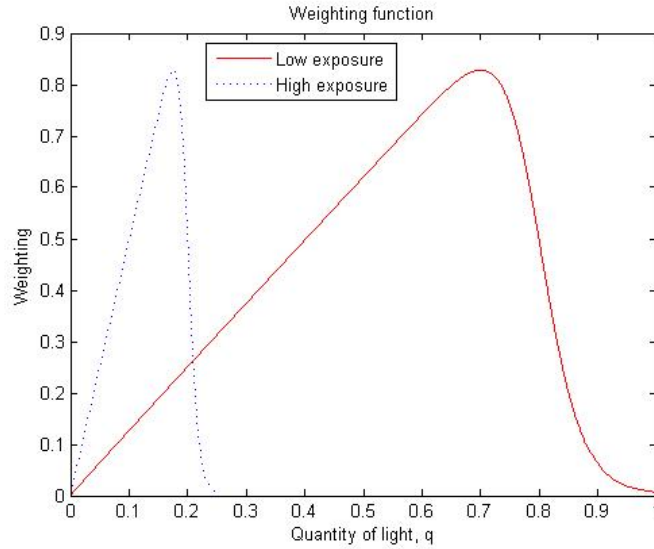


**Fig. 4-5** The weighting functions of q domain.



**Fig. 4-6** The weighting image of Fig. 4-4 (a) which is normalized to 8-bits.

**(c)The improved method:**

Considering the property of this weighting curve which is that dark side (lower q) is smooth and bright side (high q) is steep, inverting this curve could improve the issue of sharpness we discussed. Moreover, lowering the weighting of high exposure could reduce the effect of discontinuity, and lowering by 5 times was the optimal option for our experiments. Our improved weighting function and weighting image of Fig. 4-1(a) are shown in Fig. 4-7 and 4-8 respectively.

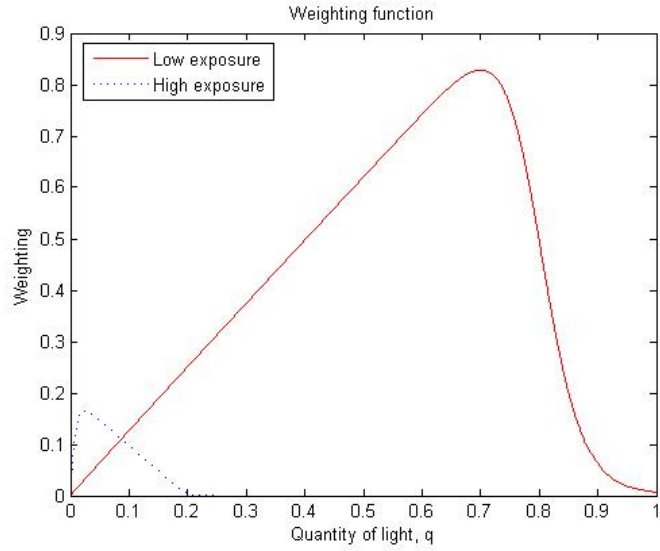


**Fig. 4-7 Our improved weighting functions of q domain.**



**Fig. 4-8 Our improved weighting image of Fig. 4-1(a) which is normalized to 8-bits.**

### **4.2.3 Combination:**

#### **(a) Previous method:**

From the concept of fusion [15], combination was in q domain. As shown in **Fig. 4-9**, **Figs. 4-4 (a)** and **(b)** were fused by our improved methods including response curve and weighting function.





**Fig. 4-9 The HDR image with discontinuous region in the sky.**

**(b)Discussions:**

Theoretically, the ratio of pixel values under the same position with different exposed images is a constant  $k$ . However, the ratio of pixel values more than 4000 with high exposed image can not be kept. **Fig. 4-10** which shows two response curves of high and low exposures in  $q$  domain can be proven. Hence, the HDR image, shown in **Fig. 4-9**, is discontinuous in sky which corresponds to the bright region.

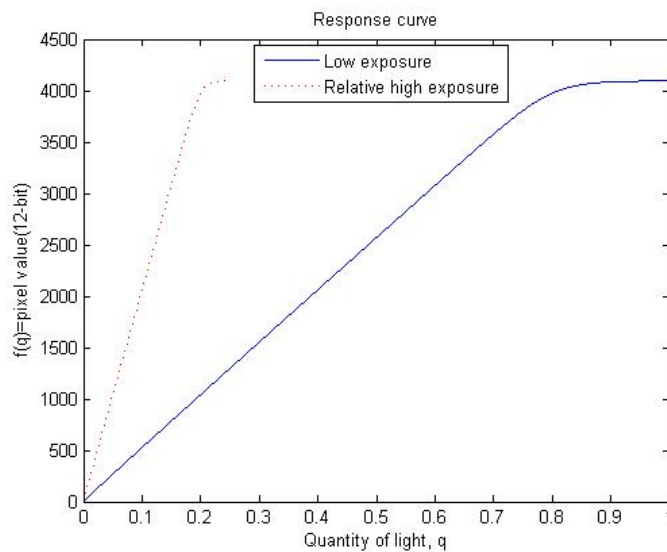


**Fig. 4-10 Two response curves of high and low exposures in  $q$  domain.**

**(c)The improved method:**

The curves of  $\log(q)$  and  $q^{1/3}$  are two substitutive curves and are all matched to the visual curve. **Fig. 4-11** shows three curves of  $q$ ,  $\log(q)$ , and  $q^{1/3}$  vs.  $f(q)$  respectively. Vertical axis presents the pixel values,  $f(q)$  and parallel axis presents the normalized range 0~1.

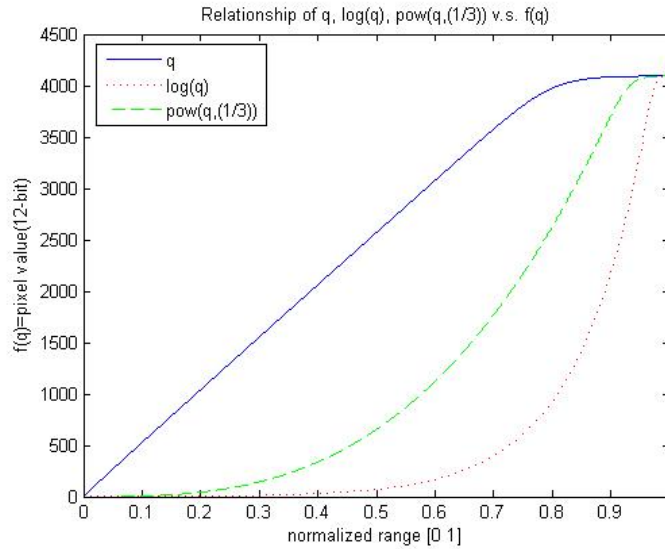


**Fig. 4-11 Three curves of  $q$ ,  $q^{1/3}$ , and  $\log(q)$  vs.  $f(q)$ .**

Although the curve  $q^{1/3}$  is a good substitution, there are still a few artifacts in bright region. On the other hand, the performance of the curve of  $\log(q)$ , such as contrast ratio and color appearance, is better than the curve of  $q^{1/3}$ . As a result, the curve of  $\log(q)$  vs.  $f(q)$  is appropriate option for our combination procedure.

### 4.3 Summary

We have already improved the main techniques including response curve, weighting function and combination of our proposed fusion algorithm. The experimental results will be given in next chapter.